$(e,2e)$ experiments on the autoionizing levels of Xe between the $^2P_{3/2}$ and $^2P_{1/2}$ ionic limits

J. G. Childers, D. B. Thompson,* and N. L. S. Martin
Department of Physics and Astronomy, University of Kentucky, Lexington, Kentucky 40506-0055
(Received 4 June 2001; published 13 November 2001)

We present $(e,2e)$ measurements of the autoionizing region of Xe between the $^2P_{3/2}$ and $^2P_{1/2}$ ionic thresholds, which correspond to ejected-electron energies of less than 1.3 eV. In an $(e,2e)$ simulation of photoelectron spectroscopy we obtain the photoabsorption spectrum and the β-parameter spectrum. The results are in fair agreement with the true photoelectron data.

DOI: 10.1103/PhysRevA.64.062703 PACS number(s): 34.80.Dp, 32.80.Dz

I. INTRODUCTION

The electron-electron coincidence or $(e,2e)$ technique has been used to investigate direct (nonresonant) electron-impact ionization in a wide variety of atomic and molecular targets [1,2]. However, the autoionization process has been systematically investigated with the $(e,2e)$ technique for only two atomic targets, He and Cd. Here we report $(e,2e)$ experiments carried out on xenon autoionizing levels.

The He experiments [3,4], carried out over a wide range of kinematic conditions, yield $(e,2e)$ energy spectra that are fitted to a generalized line-shape formula; the resulting fit parameters are compared with theoretical values. This procedure is essentially a direct comparison of measured and calculated energy spectra. Our Cd experiments [5,6] are somewhat different in concept: they rely on approximations applicable at low-momentum-transfer kinematics, which enable the isolation of interference effects between the dominant (resonant) dipole and weaker (resonant and nonresonant) nondipole processes in electron-impact ionization; magnitude and phase information are extracted from these experiments.

The autoionization spectrum of Xe between the $^2P_{3/2}$ and $^2P_{1/2}$ ionic thresholds has been extensively studied by a variety of experimental and theoretical techniques. Beutler's pioneering photoabsorption work [7] revealed two $J=1$ Rydberg series of autoionizing levels Xe $5p^5(^2P_{1/2})nd'$, ms' $(n\geqslant 6, m\geqslant 8)$ that autoionize into the Xe $5p^5(^2P_{3/2})Ed, Es$ continua, and an early calculation was carried out by Comes and Sälzer [8]. High-resolution measurements of the β parameter have been carried out by Wu *et al.* [9]; this reference also contains a survey of photoabsorption, photoionization, and photoelectron experiments. Theoretical calculations of photoprocesses were reviewed by Johnson *et al.* [10]. Less work has been done using electron-impact techniques. Geiger [11] measured the energy-loss spectrum, and LeClair and Trajmar [12] obtained the ejected-electron spectrum using a time-of-flight method; the ejected-electron energies corresponding to the autoionizing states are 0–1.3 eV.

Our long-term objective is to carry out experiments in Xe of the type carried out in Cd. The preliminary experiments reported here are designed to examine whether one of the key steps in the analysis of the Cd experiments—the isolation of the dipole component of the scattering process—is valid in Xe which, as discussed below, has a very different autoionizing region. A detailed description of our technique is given elsewhere [6,13]. In brief, the summation of pairs of $(e,2e)$ energy spectra for ejected-electron directions θ and $\theta+180°$ relative to the momentum transfer direction θ_K eliminates odd-parity angular-distribution terms which, for low momentum transfer ($K\sim 0.2$ a.u.), are mainly due to dipole-monopole and dipole-quadruple interference. [We shall refer to these spectra as summed $(e,2e)$ spectra throughout this paper.] This procedure produces an almost pure dipole spectrum that is equivalent to a photoelectron spectrum taken at the angle θ relative to the light polarization axis. In particular, the total photoelectron cross section should be mimicked by summed $(e,2e)$ spectra at the magic angle $\theta=54.7°$ [for which the second-order Legendre polynomial $P_2(\cos\theta)=0$], and the energy dependence of the photoelectron asymmetry parameter β should be derivable from the ratio of summed $(e,2e)$ spectra at two different angles. In Cd it was found that this was the case for the relatively low incident-electron beam energy of 150 eV for $(e,2e)$ experiments on the $4d^9 5s^2 5p$ autoionizing region about 12.5 eV above the ground state. A direct comparison of Cd $(e,2e)$ spectra with their true photoelectron equivalents is given in [14], and a comparison of the β parameter derived from $(e,2e)$ experiments and the true photoelectron β parameter is given in [15].

It is of interest to know whether these findings apply to xenon where the lowest-lying autoionizing levels, those between the $^2P_{3/2}$ and $^2P_{1/2}$ ionic thresholds, also lie $\sim$12.5 eV above the ground-state neutral. Because the energy loss in electron scattering is the same in the two systems, it is possible to carry out the same experiments in Xe that were done in Cd; i.e., with the same momentum transfer values and directions. However, details of the ionization process are very different for the two targets. In the Cd experiments only autoionization, and not direct ionization, is important; the process is dominated by a single configuration $4d^9 5s^2 5p$ which is excited from the $4d^{10}5s^2$ ground state by $4d \rightarrow 5p$. The *overall* process that results in the $5sEp$ continuum, with $E\sim 4$ eV, corresponds to the unperturbed value $\beta=2$ (for $5s\rightarrow Ep$) and deviations from this value are due to

*Present address: Department of Physics and Earth Science, University of North Alabama, Florence, AL 35632.

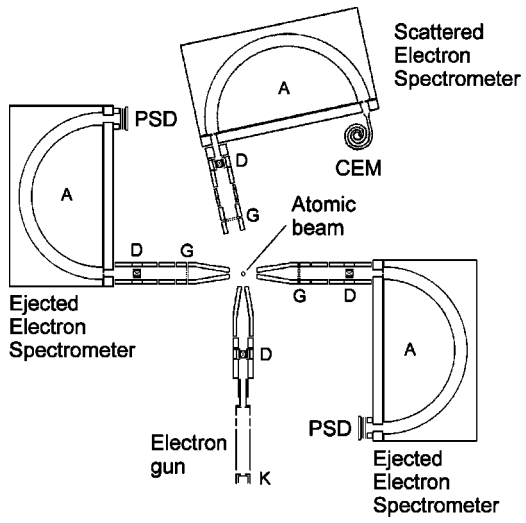

FIG. 1. Schematic of the $(e,2e)$ apparatus. *A*, hemispherical-sector energy analyzer (3 in. mean radius); *D*, deflector; *G*, grids; *K*, cathode; CEM, channel electron multiplier; PSD, position-sensitive detector.

a number of autoionizing levels that overlap and interact with the very broad $^1P_1$ level. In Xe, on the other hand, direct ionization ($5p \rightarrow Es,Ed$, where E ranges from threshold to 1.3 eV) and autoionization to two Rydberg series of levels ($5p \rightarrow nd',ms'$) are equally important. For direct ionization the unperturbed values are $\beta=1$ for $5p \rightarrow Ed$ and $\beta=0$ for $5p \rightarrow Es$; the spectral variation of β is due to the autoionizing resonances embedded in the direct ionization continua. Lastly, we note that the Cd autoionizing levels can be given approximate *LS*-coupling labels but the Xe levels require a *jj*-coupling description. Thus it is not possible to assume that the conclusions of the cadmium experiments can be carried over into xenon and it is highly desirable to repeat the Cd experiments in Xe.

Our $(e,2e)$ experiments are described below. Section II gives details of the experimental setup and Sec. III gives the results and their analysis.

II. EXPERIMENT

A schematic of the apparatus used in the present experiments is shown in Fig. 1. It is an extensively modified version of that used in the earliest Cd experiments [16]. The original configuration of an incident-electron monochromator and ejected- and scattered-electron analyzers has been replaced by one with an unmonochromated electron gun, a scattered-electron analyzer, and two identical ejected-electron analyzers mounted 180° apart on the same turntable; all these elements are coplanar and all analyzers are hemispherical-sector electrostatic types. (We will use the same convention as in Ref. [16]: for the ejected- and scattered-electron detectors angles are positive when measured clockwise from the incident electron beam direction, and negative when measured counterclockwise. We will also refer to the two ejected-electron detectors as *left* and *right*.) The gas beam effuses through a 1-mm-diameter aperture approximately 2 mm below the interaction region. The scattered electron is detected with a high-count-rate channeltron. Both ejected-electron energy analyzers contain resistive anode position-sensitive detectors (PSD's) that are connected to the same position-decoding electronics (PDE). The configuration is such that two nonoverlapping half-inch-diameter images are produced on the one-inch-diameter active area of the anodes. This technique works well and represents a considerable saving over using two PDE's. Thus two ejected-electron spectra, at angles 180° apart, can be taken simultaneously; the spectra are tagged by the position given by the PDE. Spectrometer control and data acquisition and analysis are handled by microcomputer; the software and hardware are similar to those on the $(e,2e)$ spectrometer used in recent Cd experiments [6]. As was the case in those experiments, the output from the PSD electronics triggers an interrupt pulse which provides a high-quality noncoincident ejected-electron spectrum in addition to the $(e,2e)$ spectrum obtained from the timing electronics. The noncoincident spectrum is used for alignment and normalization purposes, as described below. During an experiment energies are scanned repetitively to minimize the effect of any drift in, for example, the electron beam intensity. In the present experiments the coincidence count rates were approximately 5 counts/s at an energy resolution of about 40 meV. At the $6d'$ resonance energy the corresponding ejected-electron energy is only 0.3 eV and contact potential differences (or the charging up of surfaces) can adversely affect the spectra. Empirically we have found that a potential of 0.6 V applied to (the normally grounded) nose cones of both ejected-electron spectrometers corrects for these effects. This is discussed in more detail below. Another consequence of the low ejected-electron energies is that the drift time from the interaction region to the entrance of the electron optics (2.5 cm) is a strong function of energy that has to be accurately determined for the coincidence timing window.

The photoelectron asymmetry parameter β is obtained from our $(e,2e)$ experiments as follows. The summation of pairs of $(e,2e)$ energy spectra, for ejected electron directions θ and $\theta+180°$ relative to the momentum transfer direction θ_K, results in a dipole spectrum proportional to the differential cross section,

$$I(E,\theta) \propto \sigma(E,\theta) = \frac{\sigma(E)}{4\pi}[1+\beta(E)P_2(\cos\theta)]. \qquad (1)$$

As stated above, the form of the total photoelectron cross section $\sigma(E)$ can be obtained from a measurement at the magic angle $\theta=54.7°$ for which the second-order Legendre polynomial P_2 vanishes. The energy (E) variation of β can be obtained from measurements at two angles θ_1 and θ_2:

$$\beta = \frac{R-1}{P_2(\cos\theta_1) - RP_2(\cos\theta_2)}, \qquad (2)$$

where $R=I(E,\theta_1)/I(E,\theta_2)$.

Compared to a true photoelectron experiment [9] our energy resolution of 0.04 eV is relatively poor. The cross sections measured are thus the energy-averaged quantities

$$\overline{\sigma}(E,\theta)=\int \sigma(E',\theta)g(E-E')dE', \tag{3}$$

where $g(E-E')$ is the normalized instrument function—in the present experiments a Gaussian of 0.04 eV full width at half maximum.

Substitution of the energy-averaged cross sections in Eqs. (1) and (2) defines an energy-averaged asymmetry parameter

$$\overline{\beta}=\frac{\int \beta(E')\sigma(E')g(E-E')dE'}{\int \sigma(E')g(E-E')dE'}. \tag{4}$$

Thus we measure an asymmetry parameter which is the true asymmetry parameter weighted with the total cross section and folded with the instrument function. Notice that the form of $\overline{\beta}$ does not depend on the angles θ_1 and θ_2 at which the measurements are made.

III. RESULTS AND ANALYSIS

A. Test I: Angular distribution of noncoincident ejected-electron spectra

In order to test the validity of spectra obtained with the correcting potential on the spectrometer nose cones we examined the symmetry of noncoincident ejected-electron spectra for left-right directions $\pm\theta$ with respect to the electron beam direction and the *asymmetry* of spectra for forward-backward directions $90°\pm\theta'$; the latter property is due to odd-parity interference terms in a partial-wave expansion of the ejected-electron probability distribution [6].

Figure 2 shows three pairs of ejected-electron spectra labeled $A-F$; the left and right of each pair correspond to spectra taken in a single experiment with the pair of detectors. From symmetry we expect A and F to be the same since (to within 2°) they were taken at $\pm\theta$. Similarly, we expect B to be the same as E, and C to be the same as D. (Any differences can be ascribed to differences in the secondary-electron background; this should, however, be a smooth function of energy.) From asymmetry we expect A to be different from B, and E to be different from F. All these points appear to be true for the spectra. This can most easily be seen by examining the minimum at ~0.6 eV that lies between the $8s'$ and the $7d'$ energies; this minimum is identical and flat bottomed for $-54°$ and $+56°$, and identical and sharp for $+126°$ and $-124°$. For $\pm 90°$ the minimum is of intermediate character. From the above symmetries and asymmetries we conclude that the angular distribution is undistorted by the nose-cone potential. However, since any electric field produced by the nose-cone potentials (with respect to the gas-beam nozzle) rotates with the ejected-electron detector it is possible that the nose-cone potential increases the acceptance angle of the detector. [We attempted to find the reason for the necessity of the correcting potentials on the nose cones by carrying out a small series of experiments. Rather than applying a positive potential to the nose cones, in separate experiments we (a) applied a negative potential to the gas-beam nozzle, (b) surrounded the interaction region with a cylindrical shield (with holes at the nose-cone positions) at a positive potential, and (c) grounded the nose cone and applied a positive potential to the first mesh. None of these enabled us to obtain ejected-electron spectra at low energies. Investigations are continuing.]

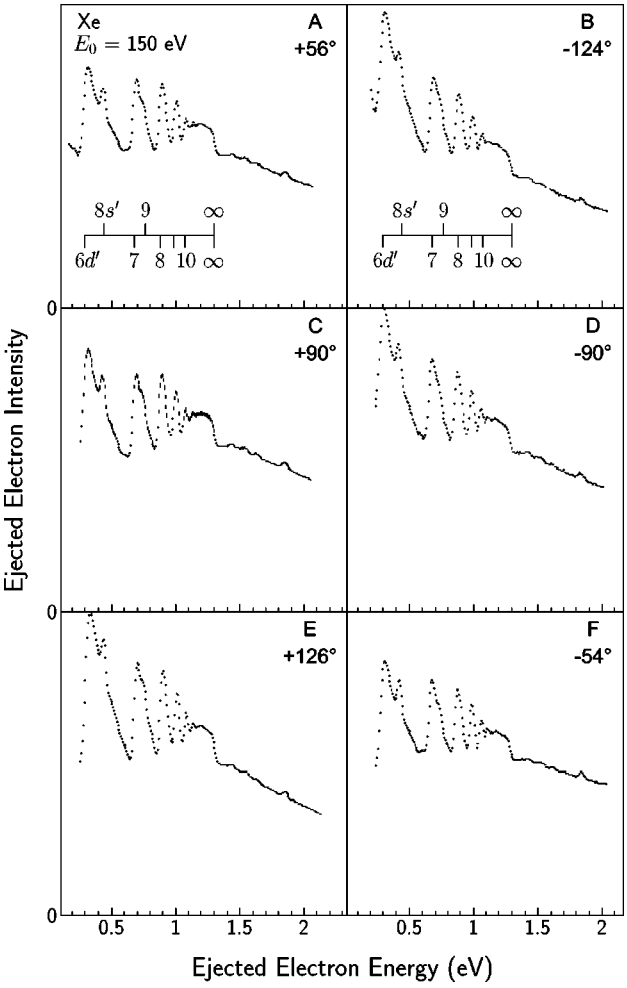

FIG. 2. Test of the apparatus using noncoincidence ejected-electron spectra for 150 eV incident-electron energy. See text for explanation. The Xe autoionizing resonances are labeled.

Lastly, we note two features in Fig. 2. First, there is a sharp drop in intensity at the $^2P_{1/2}$ ionic threshold; this also appears in the $(e,2e)$ spectra. The finite slope is due to our energy resolution of 40 meV. Secondly, above this threshold there are a number of resonances, the most prominent of which is a sharp feature at about 1.85 eV. These may be related to the *NOO* Auger transitions below 2 eV observed in photoionization by Becker *et al.* [17].

B. Test II: $(e,2e)$ spectra at 350 eV incident energy

The aim of the present experiments is to explore whether 150 eV incident energy is sufficiently high to obtain a dipole spectrum, and thus it is necessary to have confidence that the shape of energy spectra are not influenced by the nose-cone potentials. Figure 3 shows a summed $(e,2e)$ spectrum for an incident energy of 350 eV and kinematics close to the magic angle. At this energy we expect the dipole term to dominate. Hence this spectrum is a test for distortion of energy spectra by the nose-cone potentials. Since we want to compare this

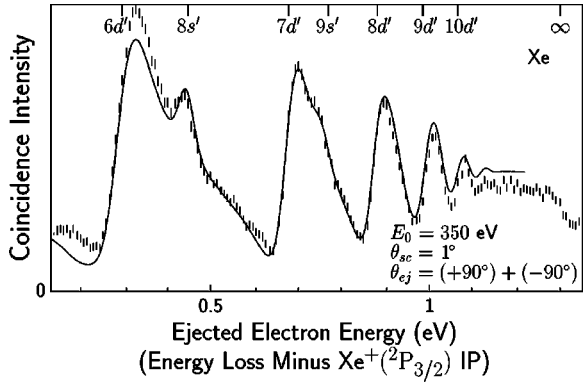

FIG. 3. Xe $(e,2e)$ spectrum for 350 eV incident energy and magic-angle kinematics. The vertical bars represent the statistical uncertainties in the data. The solid line is the true photoelectron magic-angle spectrum of the $6d',8s'$ region [9] extended to higher Rydberg levels (see text) and folded with our energy resolution of 40 meV; the curve has been normalized and energy aligned in the $7d'$ region.

spectrum with the true photoelectron magic-angle spectrum, but only the $6d',8s'$ region is available [9], we constructed the full spectrum by using the periodic formula of quantum defect theory; for details see Eqs. (3) and (4) of Ref. [18]. This ''experimental'' magic-angle photoelectron spectrum folded with our energy resolution of 40 meV is shown in the figure, with the overall intensity scaled to correspond with our results. From the good agreement of resonance positions, relative heights, and widths, we deduce that our spectra are accurate to within 10%.

C. $(e,2e)$ spectra at 150 eV incident energy

Figure 4 shows a magic-angle summed $(e,2e)$ spectrum for 150 eV incident energy, a scattering angle $\theta_{sc}=2°$, ejected-electron directions $\theta_{ej}=+90°,-90°$, and a resolution of 40 meV. This spectrum is compared with the same dipole cross section (the ''experimental'' magic-angle photoelectron spectrum) used in Fig. 3 (solid line). It can be seen

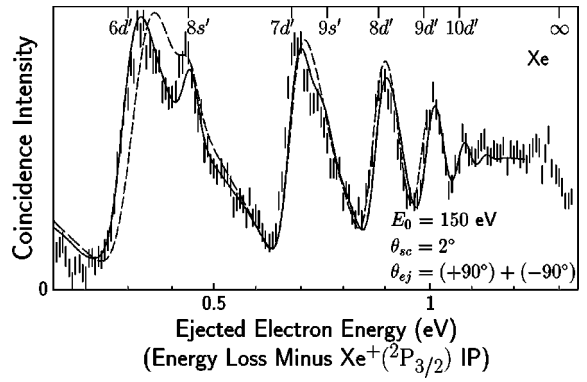

FIG. 4. Xe $(e,2e)$ spectrum for 150 eV incident energy and magic-angle kinematics. The vertical bars represent the statistical uncertainties in the data. The solid line is the same photoelectron magic-angle spectrum [9] shown in Fig. 3. The dashed line is the theoretical calculation of Johnson *et al.* [10] folded with our energy resolution of 40 meV.

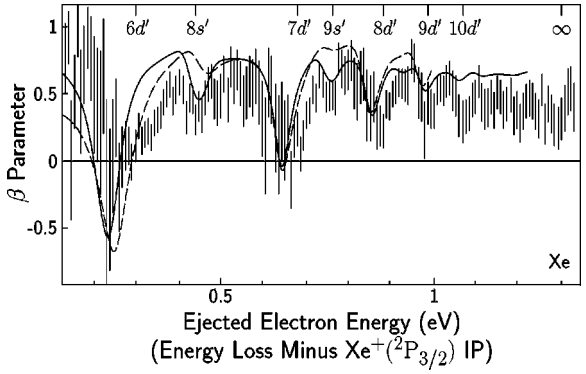

FIG. 5. The Xe β-parameter spectrum obtained from $(e,2e)$ experiments at 40 meV resolution. The vertical bars represent the combined statistical uncertainties in the data. The solid line is the true photoelectron β-parameter spectrum of the $6d',8s'$ region [9] extended to higher Rydberg levels and folded with our energy resolution of 40 meV (see text). The dashed line is the theoretical calculation of Johnson *et al.* [10] folded with our energy resolution.

that at 150 eV the summed $(e,2e)$ spectrum faithfully reproduces the dipole cross section. Also shown in the figure is the calculated photoabsorption cross section from Ref. [10] folded with our energy resolution (dashed line). Even with our relatively poor energy resolution it can be seen that our data are in much better agreement with the true photoelectron result than is the calculation.

The β parameter may be obtained from summed $(e,2e)$ spectra from two experiments carried out for θ_1,θ_2 with respect to the momentum transfer axis [see Eq. (2)]. Figure 5 shows the β parameter $\overline{\beta}$ derived from $(e,2e)$ experiments at $\theta_{sc}=0°$ (for which $K=0.15$ a.u., $\theta_K=0°$), and $\theta_1=55°,\theta_2=90°$. (With the present spectrometer configuration, 55° is the smallest accessible angle for the ejected detectors when the scattered detector is at 0°.) Since the apparatus is stable over a period of at least a day we were able to normalize the two experiments by using the last five scans of the first experiment and the first five scans of the second experiment; the two experiments were carried out sequentially over a total period of about 20 days (one scan lasts about 40 min). The normalization involves two steps: the normalization of spectral pairs for θ_n and $\theta_n+180°$ $(n=1,2)$ in order to form the summed $(e,2e)$ spectra, and the normalization of the two summed spectra to form the ratio $R=I(E,\theta_1)/I(E,\theta_2)$. In forming the ratio R it is crucial to align the energy scales of the two summed $(e,2e)$ spectra. This was achieved to better than 5 meV by using the sharp step in the $(e,2e)$ spectra at the $^2P_{1/2}$ ionization limit. (Note that the β-parameter measurement depends only on ratios of spectra taken with the same detectors at different angles and is therefore insensitive to possible distortions in the energy spectra.)

In spite of good statistics in the $(e,2e)$ spectra, the statistical uncertainties in $\overline{\beta}$ are quite large: Eq. (2) for our geometry gives $\beta\approx 2(R-1)/R$. When $|\beta|$ is small R is close to unity and a relatively small uncertainty becomes magnified in the resulting β. Our $(e,2e)$-derived $\overline{\beta}$ is compared with the true photoelectron β (solid line [9]), and a theoretical calculation (dashed line [19]), both folded with our energy

resolution by using Eq. (4) with the appropriate experimental and theoretical cross sections. Our results are in quite good overall agreement with the photoelectron data; in particular, the positions of the minima and the range of $-0.5<\overline{\beta}<+0.75$ agree well. The worst agreement is in the region of the d' resonance positions; notice that this is identical for all the resolvable Rydberg levels $6d' \rightarrow 9d'$. On the other hand, the minima at the $8s'$ and $9s'$ positions agree well with the photoelectron result and confirm the disagreement with the theoretical curve in this region.

IV. CONCLUSIONS

We have carried out $(e,2e)$ analogs of photoelectron experiments to obtain the xenon photoabsorption and β-parameter spectrum in the autoionizing region. The results obtained for the photoabsorption spectrum and the β-parameter spectrum at the relatively low incident-electron energy of 150 eV are in quite good agreement with the true photoelectron counterparts. Thus it appears that our technique of adding $(e,2e)$ spectra to eliminate nondipole ionization amplitudes (mainly monopole and quadruple for small momentum transfer) is as valid in xenon as it is in our cadmium experiments.

Experiments in xenon are under way to investigate the possibility of measuring interference terms between monopole, dipole, and quadrupole ionization amplitudes, as was done in Cd [6].

ACKNOWLEDGMENT

This work was supported by the U.S. National Science Foundation under Grant No. PHY-9987861.

[1] A. Lahmam-Bennani, J. Phys. B **24**, 2401 (1991).
[2] M. A. Coplan, J. H. Moore, and J. P. Doering, Rev. Mod. Phys. **66**, 985 (1994).
[3] A. Crowe, D. G. McDonald, S. E. Martin, and V. V. Balashov, Can. J. Phys. **74**, 736 (1996).
[4] M. J. Brunger, O. Samardzic, A. S. Kheifets, and E. Weigold, J. Phys. B **30**, 3267 (1997).
[5] N. L. S. Martin, D. B. Thompson, R. P. Bauman, and M. Wilson, Phys. Rev. Lett. **72**, 2163 (1994).
[6] N. L. S. Martin, D. B. Thompson, R. P. Bauman, and M. Wilson, Phys. Rev. A **50**, 3878 (1994).
[7] H. Beutler, Z. Phys. **93**, 177 (1935).
[8] F. J. Comes and H. G. Sälzer, Phys. Rev. **152**, 29 (1966).
[9] J. Z. Wu, S. B. Whitfield, C. D. Caldwell, M. O. Krause, P. van der Meulen, and A. Fahlman, Phys. Rev. A **42**, 1350 (1990).
[10] W. R. Johnson, K. T. Cheng, K.-N. Huang, and M. Le Dourneuf, Phys. Rev. A **22**, 989 (1980).
[11] J. Geiger, Z. Phys. A **282**, 129 (1977).
[12] L. R. LeClair and S. Trajmar, J. Phys. B **29**, 5527 (1996).
[13] N. L. S. Martin, R. P. Bauman, and M. Wilson, Phys. Rev. A **59**, 2764 (1999).
[14] N. L. S. Martin, D. B. Thompson, R. P. Bauman, M. Wilson, J. Jiménez-Mier, C. D. Caldwell, and M. O. Krause, J. Phys. B **27**, 3945 (1994).
[15] N. L. S. Martin and D. B. Thompson, J. Phys. B **25**, 115 (1992).
[16] N. L. S. Martin, T. W. Ottley, and K. J. Ross, J. Phys. B **13**, 1867 (1980).
[17] U. Becker, D. Szostak, H. G. Kerkhoff, M. Kupsch, B. Langer, R. Wehlitz, A. Yagishita, and T. Hayaishi, Phys. Rev. A **39**, 3902 (1989).
[18] K. Maeda, K. Ueda, and K. Ito, J. Phys. B **26**, 1541 (1993).